to the experimental conditions for the crystals A, B and C, respectively.

The limited instrument resolution, however, implies that the measurements were carried out using a wavelength band rather than a well defined wavelength. From the instrument parameters $\alpha_1 = 20'$ (collimation of the white neutron beam), $\beta_0 = 12'$ (mosaic spread of the monochromator) and $\alpha_2 > (\alpha_1^2 + 4\beta_0^2)^{1/2}$ (collimation between monochromator and sample) the wavelength spread per scan point can be estimated (see, for example, Kalus & Dorner, 1973). The resulting smearing in A is indicated by the full lines above and below the dotted line in Fig. 7 and it is listed in Table 5, expressed as $\Delta A/\pi$. For $\Delta A/\pi < \pm\frac{1}{2}$ the average value of R_H^y depends on the exact value of A_0, the mean A value. Assuming that A_0 is known only within an uncertainty of $\pm\pi/2$, we calculated the maximum deviation of R_H^y, averaged over the ΔA range, from the mean value $R^y_{\text{mean}} = \pi/2$. From these deviations, expressed as $\Delta R^y/R^y_{\text{mean}}$ in Table 5, the errors S_{osc} listed in Table 3 were derived. The S_{osc} values represent the maximum errors introduced into α by the oscillations of R_H^y.

References

ALDRED, P. J. E. & HART, M. (1973). *Proc. R. Soc. London Ser. A*, **332**, 223–254.

BÄRNIGHAUSEN, E. (1978). *J. Appl. Cryst.* **11**, 221–228.

BRUGGER, R. M. (1976). *Nucl. Instrum. Methods*, **135**, 289–291.

COOPER, M. J. (1971). *Acta Cryst.* A**27**, 148–157.

COPPENS, P. (1974). *LINEX*. Chemistry Department, State Univ. of New York at Buffalo, Buffalo, New York 14214, USA.

FREUND, A. (1980). Internal scientific report, Institut Laue–Langevin, Grenoble, France.

HAYTER, J. B., LEHMANN, M. S., MEZEI, F. & ZEYEN, C. M. E. (1979). *Acta Cryst.* A**35**, 333–336.

KALUS, J. & DORNER, B. (1973). *Acta Cryst.* A**29**, 526–528.

LARSEN, F. K., LEHMANN, M. S. & MERISALO, M. (1980). *Acta Cryst.* A**36**, 159–163.

MCSKIMIN, H. J. (1953). *J. Appl. Phys.* **24**, 988–997.

MERISALO, M. & KURITTU, J. (1978). *J. Appl. Cryst.* **11**, 179–183.

NILSSON, N. (1957). *Ark. Fys.* **12**, 247–257.

O'CONNOR, D. A. & BUTT, N. M. (1963). *Phys. Lett.* **7**, 233–235.

RAUCH, H. & PETRASCHECK, D. (1978). In *Neutron Diffraction*, edited by H. DACHS, pp. 303–351. Berlin–Heidelberg–New York: Springer.

SEEGER, R. J. & TELLER, E. (1942). *Phys. Rev.* **62**, 37–40.

SHULL, C. G. & OBERTEUFFER, J. A. (1972). *Phys. Rev. Lett.* **29**, 871–874.

WILLIS, B. T. M. (1969). *Acta Cryst.* A**25**, 277–300.

WILLIS, B. T. M. (1970). *Acta Cryst.* A**26**, 396–401.

ZACHARIASEN, W. H. (1945). *Theory of X-ray Diffraction in Crystals*. New York: John Wiley.

ZASIMOV, V. S., LOBANOV, N. N., RÜBIGER, J. & KUSMIN, R. N. (1976). *Phys. Status Solidi A*, **38**, K45–K47.

Acta Cryst. (1981). A**37**, 871–875

Investigation of Long-Range Order in Protein Crystals by X-ray Diffraction

BY A. SHAIKEVITCH AND Z. KAM

Polymer Department, The Weizmann Institute of Science, Rehovot, Israel

(*Received* 21 *January* 1981; *accepted* 5 *May* 1981)

Abstract

The rate and mechanisms of growth and the final quality of crystals are related to lattice disorders and can be studied from the analysis of X-ray diffraction patterns. Crystals of proteins and other biological macromolecules display features which are different from those of inorganic crystals. In this work the long-range order of protein crystals is probed *via* the mosaic spread, with a special camera constructed for this purpose. The very small mosaic spread measured indicates almost perfect long-range order in the crystal, suggesting the absence of dislocations. This is compatible with the weak binding energies and mechanical softness of protein crystals. If indeed such crystals do not incorporate dislocations, accumulation of strain may be a possible mechanism for the cessation of growth of protein crystals. Microscopic observations of crystal growth support this idea.

0567-7394/81/060871-05$01.00

Introduction

The determination of the three-dimensional electron density of macromolecules from X-ray crystallography is limited in its resolution by the decrease in intensities of high-order diffraction peaks due to the size and quality of the crystal and the nature of the crystallized molecule. The mosaic spread and temperature factors are conventionally used to describe the effect of long- and short-range disorders on the intensity and the width of diffraction peaks (James, 1965; Alexander & Smith, 1962).

The mosaic picture was established first for inorganic crystals, and is described by perfect lattice domains bounded by dislocations (Auleytner, 1964). Intuitively, impurities in biological preparations, the structural and chemical heterogeneity of the soft and conformationally variable macromolecules, and the low binding energies of proteins in crystals, all support a different, more continuous picture for deviations from the ideally perfect crystal.

For three-dimensional lattices one often relates the growth of thin plates or elongated needle-like crystals to stronger bonding of the molecules in the direction of the long axis of the crystals, which may imply better fitting and longer range of order in these orientations. On the other hand, growth may be accelerated by dislocations, which creates lattices with poor long-range order.

The growth of protein crystals is often hindered, and the cessation of the growth results in very small crystallites. In previous work (Kam, Shore & Feher, 1978) regrowth on surfaces of cleaved crystals was found. This suggested that growth is affected by accumulation of errors in the lattice as the crystal becomes larger. The role of dislocation in growth and final quality of protein crystals is unknown. Since the density of dislocations can be probed *via* the mosaic spread we are interested in such measurements. The determination of the mosaic spread as a function of position across a protein crystal might shed light on the disorder on the surface and in the bulk of these crystals in different stages of their growth

To perform these measurements, a special X-ray camera was constructed and used. It was designed to be able to measure the rocking curves of reflexions from extremely well ordered crystals with negligible contribution of incident beam divergence, yet with reasonable flux. The camera is described in the next section. In the following section, the results are reported and discussed.

Design considerations and description of the camera

The profile of a diffraction peak is a convolution of several contributions. We first evaluate each of these contributions in order to be able to control experimentally the effect of the different parameters on the measured profile of a reflexion, and minimize instrumental broadening while still keeping the intensity of the incident X-ray beam sufficient for a reasonable counting rate of diffracted photons. Since the mosaic spread we measured was very small, the parameters were optimized to overcome this problem.

In order to reduce the instrumental contributions to the 'angular' width of the reflexions below the mosaic spread, a small-angle X-ray scattering camera configuration is used. The camera has collimation length up to 750 mm. A linear position-sensitive detector (Tennelec PSD 100) records the reflexions and their position. A multichannel analyzer (Intertechnique SA 40) accumulates the position histogram. Since the detector is 'one-dimensional', with vertical aperture of 4 mm, one has to rotate the crystal perpendicular to the incident beam so as to bring the reflexion of interest to the horizontal plane. The linear resolution of the detector is about 0·2 mm.

The source is a line focus on a Cu target electrode surface 'seen' from about 6° (Philips 1·2 kW fine-focus X-ray tube RDF 50/1). The effective source size is 0·04 × 8 mm. The horizontal and vertical divergence of X-ray beams passing through the extreme ends of the slits is given by simple geometry (see Fig. 1 for definition of symbols):

$$\gamma_H = \left\{ \frac{0{\cdot}04 + S_2^H}{2d'} \right\} \tag{1}$$

and

$$\gamma_V = \mathrm{MIN} \left\{ \frac{S_1^V + S_2^V}{2d}; \frac{S_2^V}{2d''}; \frac{S_1^V}{2(d + d'')} \right\}, \tag{2}$$

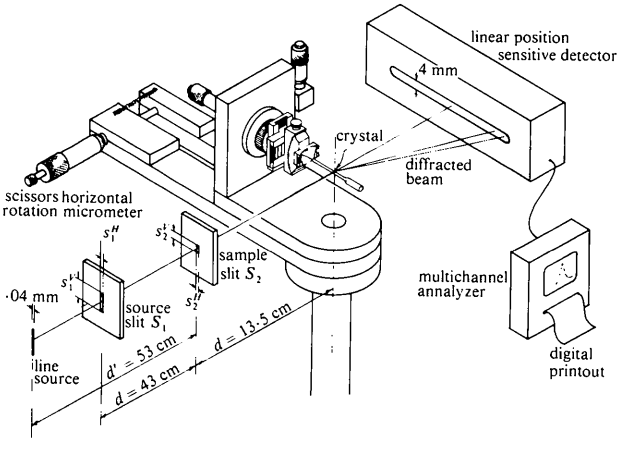

Fig. 1. Schematics of the camera used for measuring angular width of reflexions. The different goniometric adjustments of the crystal tube are used to position the crystal in the beam and bring the reflexion to lie in the horizontal plane. The micrometric scissors are used to scan the reflexion rocking curve by fine adjustment of the crystal horizontal angle.

where MIN indicates the smallest of the values in the brackets.

Since β is much less sensitive to vertical divergence of the beam, we gain intensity by using the long and the very thin line source, while still keeping horizontal divergence smaller than the mosaic spread.

The crystal was mounted in a quartz tube on a standard one-circle centerable goniometer stage which was attached to a base in the form of long micrometric scissors rotated in the horizontal plane (Fig. 1). In order to measure the rocking curve of reflexions, the diffraction peak was first brought onto the detector and optimized to fall in the horizontal plane at the middle of the detector vertical aperture. Then the angle between the crystal and the incident X-ray beam was scanned in small steps by rotation in the horizontal plane, with the micrometric scissors. For each crystal orientation, the diffraction peak intensity was integrated over all the position channels after background was subtracted. By plotting integrated intensity as a function of scissors angle, detector resolution, crystal size and beam size did not affect the results. In order to measure reflexions from a small part of the crystal, the second slit was replaced by a pinhole.

Materials

Egg-white lysozyme was purchased from Worthington. The lypholized powder was dissolved in pH 4·2, 0·1 *M* sodium acetate/acetic acid buffer. 6% stock solution was mixed in equal volumes with 8% NaCl in the same buffer, passed through 0·22 μm millipore filters and left for a few days. Crystals appeared within a day and continued to grow for about a week.

Chymotrypsin from Sigma was dissolved in pH 4·2 citrate buffer. 0·5 to 1 ml of 4% stock solution was placed in a dialysis bag inside a beaker filled with 10 ml of about 50% $(NH_4)_2SO_4$ solution in the same buffer. After a few weeks big and thick plates of chymotrypsin crystals (0·5 × 4 mm) grew in some bags.

Horse-heart myoglobin from Sigma was dissolved in 0·1 *M* pH 6·8 phosphate buffer, centrifuged, millipore filtered and mixed with three volumes of saturated ammonium sulfate solution. Crystals grew within a few days.

Selected crystals were chosen from the crystallization dish and mounted in a standard X-ray quartz capillary. The mother liquor was removed around the crystal to minimize background scattering and a drop was left in the capillary away from the X-ray beam path to prevent drying of the crystal.

Experimental results

Two examples of profiles of a diffraction peak from a lysozyme crystal at $2\theta \simeq 15°$ as a function of the angle of the micrometric scissors are shown in Fig. 2 for two extreme settings of collimation slits. If one approximates the different contributions to the diffraction profiles by Gaussians, the measured profile is the convolution of these contributions, and the squares of angular widths of the contributions are added up to give the measured profile width squared. This is confirmed in Fig. 2(*c*). The extrapolated contribution for vanishing beam divergence gives a contribution of the crystal mosaic spread of ~0·3 mrad. For a 0·1 mm slit (Fig. 2*b*), the contribution of the beam divergence is less than 10% of the total profile width. The separability of the Cu $K\alpha$ doublet makes the contribution of monochromatization width negligible. Similar values for the mosaic spread were found with synchrotron radiation (Phillips, 1978).

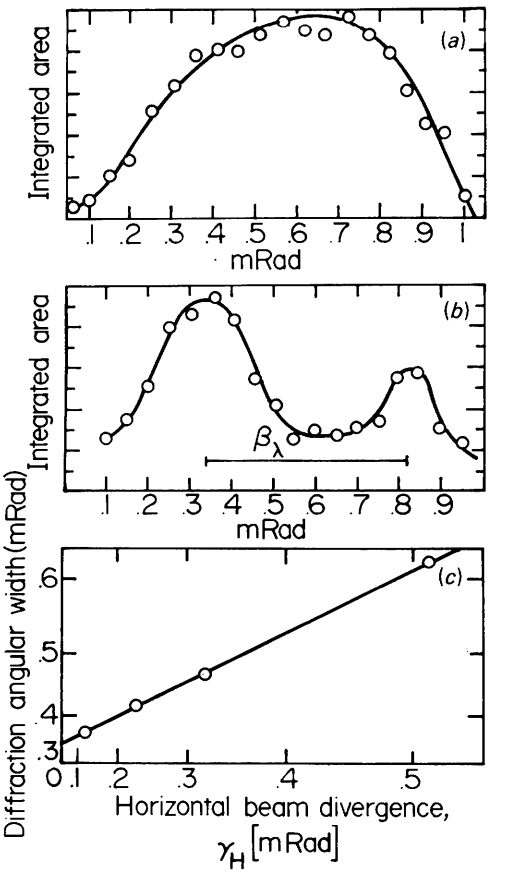

Fig. 2. The rocking curves of a reflexion of a lysozyme crystal for different values of beam divergence. Each data point presents background-subtracted integrated intensity in a still picture on the position-sensitive detector. The plots as a function of crystal horizontal angle are given for the two extreme values of the beam divergence used. (*a*) 0·5 mm sample slit width corresponding to $\beta_H = 0{\cdot}001 \gg \beta_v, \beta_\lambda$; (*b*) 0·1 mm sample slit, corresponding to $\beta_H = 0{\cdot}0003$, $\beta_v = 0{\cdot}0001$, $\beta_\lambda = 0{\cdot}0005$. The two separable peaks correspond to the $K\alpha_1$ and $K\alpha_2$ doublet in the Cu $K\alpha$ line; (*c*) the relation between the squares of the angular width β and the beam divergence γ_H, confirming the linear relationship between them. The extrapolation to zero beam divergence determines the mosaic spread.

The profile of the same diffraction peak as a function of position on the crystal was measured by moving a pinhole in front of the crystal. Intensities were normalized to the volume of the crystal that diffracts, as measured from absorption of the direct beam. The integrated intensities and the mosaic spread were independent of position within experimental error. The mosaic spread was also measured as the crystal was allowed to dry out. Although the diffraction moved, reflecting a shrinking unit cell, no apparent broadening was detected until a very fast disappearance of the diffraction occurred.

We attempted to measure the profile from a small fragment of the crystal taken from the center after carefully cutting the original large crystal to pieces. The width of the profile and the multipeak structure indicate that the cutting damaged the lattice.

The mosaic spread of a large (10 mm) myoglobin crystal was also measured. The crystal was twinned, and several sharp reflexions, each with mosaic spread of less than 0·5 mrad, spanned a rocking curve with a total width of about 2 mrad.

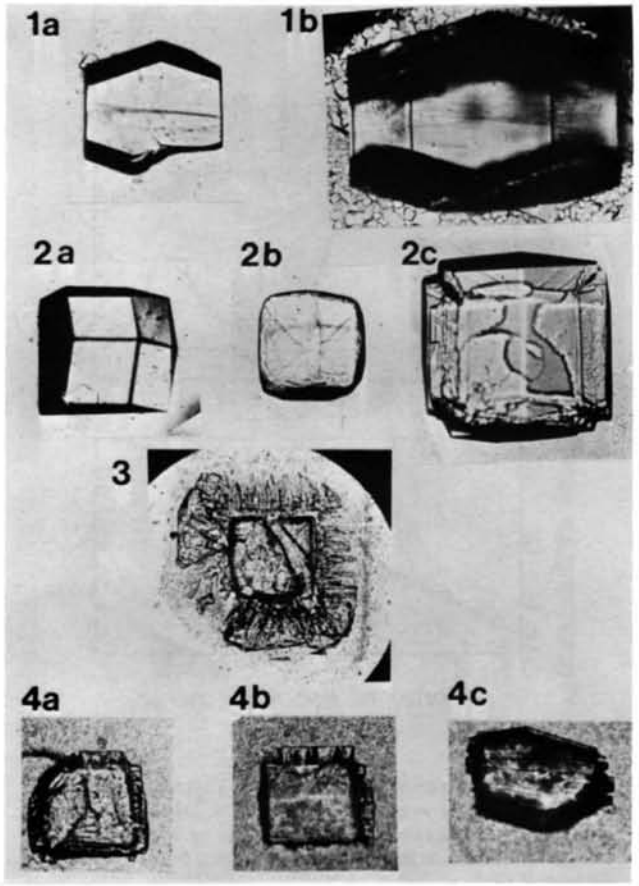

Fig. 3. Plate 1. Enlarged photographs of a regrown crystal following a short wash in undersaturated mixture: (*a*) original; (*b*) regrown. Plate 2. Photograph of a regrown crystal following etching in a flow of undersaturated mixture: (*a*) original; (*b*) etched; (*c*) regrown. Plate 3. Photograph of an intermediate stage in the process of etching a regrown crystal in undersaturated mixture. Plate 4. Photographs of crystals slowly regrown following replacement in fresh crystallization mixtures.

Since many protein crystals are transparent, we also studied the growth of crystals as seen by the light microscope.

In Fig. 3, plate 1, we show a crystal that was washed quickly and replaced in a new supersaturated solution. The crystal regrew considerably, yet the original crystal is seen well inside the regrown one. The newly regrown layers can be easily split mechanically from the original crystal. Fig. 3, plate 2, shows the regrowth of a crystal which was washed for a longer period and replaced in fresh solution. Although the original crystal surfaces totally dissolved, their position reappeared inside the regrown crystal. Moreover, the growth seems to be independent on each surface and does not match at the edges at all. Etching is a common technique to visualize lattice disorders for inorganic crystals. Fig. 3, plate 3, shows regrown crystals which were etched by a flow of undersaturated solution. The original crystal was much more resistant to the etching compared to the regrown layers, and the latter were etched along radial grooves (rather than by layers as in plate 2). This may imply a mode of growth of independent nucleation and growth sites on the old surface, and weaker joints between them. This mode of growth is also seen in slow regrowth of washed crystals in Fig. 3, plate 4.

Discussion

The protein crystallographer is mainly interested in short-range order as is manifested by the maximum angle of diffraction. The mosaic spread of the crystal, β, affects the maximum available resolution, d, only when $\beta \simeq d/a$, a being the unit-cell linear dimension (*e.g.* for $d = 1$ Å and $a = 100$ Å, $\beta < 10$ mrad or $0{\cdot}5°$). The mosaic spreads we measured are much smaller. We still suggest the relevance of the long-range order, as probed by the mosaic spread, to the crystal terminal size *via* the model of accumulation of errors in the lattice.

Lattice errors could be local (point impurities and vacations) or extended (like line or plane dislocations). Proteins may produce local disorder owing to their variable conformation. This was recently analyzed (Frauenfelder, Petsko & Tsernoglou, 1979; Artymiuk, Blake, Grace, Oatley, Phillips & Sternberg, 1979) from the temperature dependence of diffraction intensities. It may produce stresses and strains in the unit cell, which can add up along the lattice as the crystal grows, and relax at dislocations. There may be two ways for such errors to propagate: (1) accumulation of systematic misfits of the protein into the lattice unit cell; (2) random accumulation of statistical distribution of conformations. The lack of symmetry and the softness of the protein molecules can allow for both these 'errors'.

Systematic misfit accumulation is linearly proportional to the number of unit cells, whereas random errors grow in each direction as the square root of the number of cells. It will be plausible to assume that accumulation of strains of the order of magnitude of the unit cell result in a dislocation, *i.e.* it determines the size of the mosaic block. A missing unit cell over the length of a dislocation between two mosaic blocks of N unit cells causes a tilt angle $\beta \simeq N^{-1}$ between them. Taking a value of $\beta = 0{\cdot}3$ mrad for the mosaic spread, we find that systematic errors accumulate to one unit-cell dimension over 3000 unit cells (*i.e.* 1·2 μm mosaic block for $a = 40$ Å unit-cell length). Considering, on the other hand, a lattice with random conformations of the molecules causing random accumulation of strains, it will take N^2 unit cells to tilt a crystallographic plane by an angle β, or a whole crystal of 3·6 mm length could be free of dislocations. In the first case, it would not be clear why a crystal consisting of a huge number of dislocations would stop growing. On the other hand, the second case of random errors allows one to interpret the measured mosaic spread and the crystal's terminal size *via* a model which argues that protein crystals cannot incorporate dislocations in order to relax stresses and strains that accumulate in its growth. Indeed, the energetics of protein crystallization marginally stabilizes the crystal phase with respect to the solution (Kam, Shore & Feher, 1978). It is possible that a molecule which cannot fully bind itself inside a strained lattice would dissolve, and that the loss of binding energy around extended dislocation hinders growth around them and prevents their incorporation in the bulk of the crystal. Although it may not prevent nucleation of new crystals on the old surfaces at high enough supersaturations, these crystals do not fit to a continuous uniform lattice as observed microscopically and do not contribute to the intensity of diffraction of the main peaks.

The constant mosaic spread measured during the drying of crystals is also compatible with the lack of dislocations in the lattice. The existence of many mosaic blocks, which dehydrated differently depending on the distance from the surface, could result in their independent slippage and the broadening of diffraction angles as the unit cell shrank. The uniform shrinking of the whole crystal with no apparent broadening of the mosaic spread supports the picture of close to a perfect lattice for protein crystals.

In order to establish further the proposed ideas, the reported results have to be extended to a selection of different protein crystals of varying sizes, shapes and mosaic spreads and performed on reflexions at different Bragg angles. Topography of protein crystals has not yet been done. This approach is capable of direct visualization of dislocations in crystals (Tanner & Bowen, 1980). Protein crystals can be crosslinked, embedded in resins, and thin sections can be directly investigated by electron microscopy. However, the fixation procedures are too crude to deduce long-range order and existence of dislocations in the original lattice.

If indeed the mosaic spread of protein crystals is very small, there is an interesting application to powder-pattern structural analysis with well collimated sources since sharp well resolved rings could yield medium resolution data for proteins that did not produce large enough single crystals.

We would like to thank Professor George Feher for initiating these studies and for many stimulating discussions.

This research was supported by a grant from the United States–Israel Binational Science Foundation (BSF), Jerusalem, Israel. ZK is the incumbent of the Pollak Career Development Chair.

References

ALEXANDER, L. E. & SMITH, G. S. (1962). *Acta Cryst.* **15**, 983–1004.

ARTYMIUK, P. J., BLAKE, C. C. F., GRACE, D. E. P., OATLEY, S. J., PHILLIPS, D. C. & STERNBERG, M. J. E. (1979). *Nature (London)*, **280**, 563–588.

AULEYTNER, J. (1964). *X-ray Methods in the Study of Defects in Single Crystals.* Oxford: Pergamon Press, Warszawa: Polish Scientific Publishers.

FRAUENFELDER, H., PETSKO, G. A. & TSERNOGLOU, D. (1979). *Nature (London)*, **280**, 558–563.

JAMES, R. W. (1965). *The Optical Principles of Diffraction of X-rays.* Ithaca, New York: Cornell Univ. Press.

KAM, Z., SHORE, H. B. & FEHER, G. (1978). *J. Mol. Biol.* **123**, 539–555.

PHILLIPS, J. C. (1978). Thesis, Stanford Univ.

TANNER, B. K. & BOWEN, D. K. (1980). *Characterization of Crystal Growth Defects by X-ray Methods.* New York: Plenum Press.